Detailed Models of super-Earths: How well can we infer bulk properties?

Diana Valencia[1]

Earth and Planetary Science Dept., Harvard University, 20 Oxford Street, Cambridge, MA, 02138

valencia@mail.geophysics.harvard.edu

Dimitar D. Sasselov

Harvard-Smithsonian Center for Astrophysics, 60 Garden Street, Cambridge, MA, 02138

and

Richard J. O'Connell

Earth and Planetary Science Dept., Harvard University, 20 Oxford Street, Cambridge, MA, 02138

ABSTRACT

The field of extrasolar planets has rapidly expanded to include the detection of planets with masses smaller than that of Uranus. Many of these are expected to have little or no hydrogen and helium gas and we might find Earth analogs among them. In this paper we describe our detailed interior models for a rich variety of such massive terrestrial and ocean planets in the 1-to-10 $M_{\oplus}$ range (super-Earths). The grid presented here allows the characterization of the bulk composition of super-Earths detected in transit and with a measured mass. We show that, on average, planet radius measurements to better than 5%, combined with mass measurements to better than 10% would permit us to distinguish between an icy or rocky composition. This is due to the fact that there is a maximum radius a rocky terrestrial planet may achieve for a given mass. Any value of the radius above this maximum terrestrial radius implies that the planet contains a large ($> 10\%$) amount of water (ocean planet).

Subject headings: planetary systems — planets and satellites — Earth

[1]corresponding author

1. Introduction

A new family of exo-planets is now being explored thanks to improvements in detection methods that allow the discovery of very low mass objects (1-10 $M_\oplus$ hereinafter super-Earths). The first three super-Earths discovered are: GJ876d - a 7.5 $M_\oplus$ planet at 0.02 AU from its star (Rivera et al. 2005), OGLE-2005-BLG-390Lb - a 5 $M_\oplus$ planet at 5 AU (Beaulieu et al. 2006) and HD69830b - a $10.8M_\oplus$ at 0.08 AU (Lovis et al. 2006). In the next few years, with missions like COROT, that launched in December 2006 (Borde et al. (2003)) and *Kepler*, scheduled to launch in 2008 (Borucki et al. 2003), many more - and smaller, super-Earths are expected to be found. These missions detect planets by observing their transits, hence allow for a measurement of the planet's radius, R. The Doppler techniques have improved significantly and allow detection and planet mass, M, determination for super-Earths as well, as demonstrated by the discovery of GJ876d and HD69830b.

Our work is motivated by the need for mass-radius relations for super-Earths of varied compositions. Such relations should allow discerning the bulk compositions of planets detected in transit - with derived R and M. Zero-temperature sphere models (Zapolsky & Salpeter 1969; Stevenson 1982; Fortney et al. 2006) allow approximate mass-radius calculations for specific simple materials (pure Fe, pure olivine, pure water). Valencia et al. (2006) introduced detailed interior models for super-Earths. These models were extended to super-Earths with large water content (Valencia et al. 2007) - the ocean planets proposed by Kuchner (2003); Leger et al. (2004). A cold ocean planet model was introduced by Ehrenreich et al. (2006) for the low-temperature planet OGLE-2005-BLG-390Lb.

Distinguishing between ocean planets and dry rocky super-Earth planets is not trivial, because at a given mass the same planet radius could correspond to different mixtures of iron core, mantle minerals, and ices (Valencia et al. 2007). Observations with certain tolerances of the derived planetary R and M are required, as shown for two particular cases by Selsis et al. (2007). On the other hand, there is very strong motivation to be able to distinguish between ocean planets and dry planets, because of all the implications to planet formation theory and the development of habitable environments. Models of planet formation (Ida & Lin 2004; Rafikov 2006; Kennedy et al. 2006; Raymond et al. 2006) anticipate the formation of super-Earths with a rich variety of bulk compositions, but differ in the details.

As the field of planets with masses in the range of 1-$10M_\oplus$ emerges, it will be useful to have a consistent nomenclature to describe such planets. We propose to call a super-Earth, a planet with large amounts of solid material in the 1-$10M_\oplus$ range. The lower bound is obvious for historical reasons, the upper bound is somewhat arbitrary. It is informed by the physical argument that at $\sim 10M_\oplus$ and above, the planet can retain H and He during formation (Ida & Lin 2004). Super-Earths, includes ocean planets and massive terrestrial planets as a

subclass in this mass range. Planets with H_2O on the order of $\geq 10\%$ in either liquid and/or solid phase are termed ocean planets. Massive terrestrial planets will then be the ones with little water on the surface or in the mineral assemblages and hence, be the most similar to Earth. The existence of a large core of iron makes a difference, therefore within super-Earths there is a subset of planets with large cores that we have termed 'super-Mercuries', and which can be terrestrial or have a large ocean. The name 'ice giants' - Uranus and Neptune - has been reserved for planets more massive than $10M_\oplus$ with some amount of gas ($\sim 10\%$). In addition, it is possible, though unlikely, that planets with $M < 10M_\oplus$ could have a lot of gas ($> 10\%$), but we do not model them in this paper. At $10M_\oplus$, a complication arises due to the possibility of H and He retention by the planet during formation. We do not consider these planets in this paper as a separate class since they can be treated as massive ocean planets with high H_2O content and a relatively small layer of gas above it that would add a few kilometers to the radius. The regime of $M < 1M_\oplus$, that includes Mars, Venus, Mercury and the icy-satellites of the Solar System has been studied previously with models describing these planets and therefore has been left out of this paper.

In this study we explain how we can differentiate between a rocky and an ocean super-Earth with measurements of mass (M) and radius (R) at the current precision levels. In the first section we briefly explain the model used to obtain the internal structure of a super-Earth given its composition (χ) and M. This model has been used to determine the total radius and interior distribution of bulk parameters (mass, gravity, pressure and temperature) of terrestrial and ocean exo-planets (Valencia et al. 2006, 2007) and here we present another useful application of this model: how to obtain constraints on χ with values of M and R.

2. Model

We model the internal structure of a low mass exo-planet by dividing its interior in concentric shells where composition is considered homogenous. Within each layer the numerical model solves the standard differential equations for density, pressure, mass and gravity structure under hydrostatic equilibrium. The equation of state (EOS) chosen to relate density, pressure and temperature is the Vinet EOS (Vinet et al. 1989) that extrapolates better to high pressures than the third-order Birch-Murnaghan (BM3) EOS (Hama & Suito 1996; Cohen et al. 2000). The regions are:

- an H_2O layer divided into a water ocean over an icy shell - composed of high-pressure ices VII and X
- the mantle divided into an upper mantle - composed of olivine $([Mg_{1-x},Fe_x]_2SiO_4)^\alpha$,

wadsleyite ($[Mg_{1-x},Fe_x]_2SiO_4)^\beta$ and ringwoodite ($[Mg_{1-x},Fe_x]_2SiO_4)^\gamma$ - and a lower mantle - composed of perovskite ($[Mg_{1-x},Fe_x]SiO_3$), ferromagnesiowusite ($[Mg_{1-x},Fe_x]O$) and post-perovskite ($[Mg_{1-x},Fe_x]SiO_3$)

- and the core (mainly Fe), that can be divided into a liquid outer layer and inner solid layer if the temperature profile of the planet crosses the melting curve of iron.

The thickness of the H_2O, mantle and core regions are dependent on the ice mass fraction (IMF) and core mass fraction (CMF) that are assumed for a planet. The Earth has a negligible water fraction (IMF=0.02-0.1%) and a core that is 1/3 of its mass (CMF=32.59%, Stacey (1992)). Phase transitions are modeled in each region to obtain the different layers composing the planet. The temperature profile is modeled after the Earth's; the temperature gradient is adiabatic within each region and conductive within the boundary layers developed at the top and bottom of the mantle. The boundary layers in the H_2O and core regions are neglected owing to their very low viscosity that prevents thick boundary layers to develop. The surface temperature is taken to be 500 K after the detection of GJ876d with an estimated surface temperature of $430 - 650$K (Rivera et al. 2005). Despite this high value, water may be present provided the surface pressure is large enough ($\sim$ 1000 atm for $T_{surf} = 500$). For more details please refer to Valencia et al. (2006, 2007) where the model is explained thoroughly. Currently the models are not evolved in time; they correspond to a planet that has undergone differentiation and achieved equilibrium like our Earth.

This numerical model allows us to calculate the total radius of a planet given its mass and composition. We do not know the exact composition of the planets that will be discovered in the near future but we can make reasonable assumptions on their bulk composition. The dominant minerals in the mantle are most likely the same as for Earth (silicates with a small incorporation of iron -$\sim$10%). The core is mainly composed of Fe. The Earth's core is known to have some Ni (mostly in the inner core) and a light alloy in the outer core of $\sim$10%. The nature of the light alloy and exact amount are not known for Earth. Instead of looking at all possible candidates (O, H, S, Si, C) we model the core as pure Fe in this study and anticipate that the presence of a light allow will increase the radius by a few hundred kilometers. The water region is composed of ice VII and X. For low temperature planets, there might also be an extra icy layer of Ice I above the water ocean. This layer will be small due to the small stability field of Ice I and hence we consider the results presented in this study to be adequate even for low temperature icy planets (such as Ganymede, Europa and Calisto massive analogs). For planets that are very close to its parent star, their surface temperature might be on the order of $500 - 1500$K. Ice VII is a high pressure form of H_2O that could be the source of a liquid water layer, provided the surface temperature is high enough according to the phase diagram of H_2O (Wagner & Pruss 2002). The thermal structure has little effect

on the radius of a planet (Valencia et al. 2006) but imposes conditions on the compositional phases, particularily of H_2O at the surface. If the surface temperature is higher than the critical point (T_{crit} = 647K and P_{crit} = 218 atm) the structure of an ocean planet will vary gradually from a vapor phase to an ice VII phase at depth.

3. Ternary Diagram

We have computed a grid of interior models appropriate for ocean and terrestrial planets with the entire range of CMF and IMF to determine how M, R and χ are related. Since the percentage of mass in the mantle, ices and core has to add up to 1, we use a ternary diagram to show the results. Ternary diagrams are commonly used in Earth sciences. Data of a three-component system is plotted in a triangle whose sides depict three axes. Each vertex means 100% of a particular component and data plotted on the opposite side means 0%. Lines parallel to a particular side will show various degrees of a component whose maximum value is shown at the corresponding opposite vertex. We use a fourth axis (color code or label) to show the value for the radius for each composition. A 3-dimensional volume describes the complete family of Mass-Radius relations for all compositional combinations; a ternary diagram is a cross-section at a given mass. Figure 1 shows some examples for a $5M_\oplus$ planet (like OGLE-2005-BLG-390Lb) with three different compositions (A) CMF=10% and IMF=50% with a radius of 12200km, (B) CMF=20% and IMF=10% with a radius of 10750km , (C) CMF=30% and no water with a radius of 9800km and (D) CMF=40% and IMF=30% with a radius of 10950km.

A minimum and maximum radius exists for a planet with mass M. The smallest a planet can be is when it is composed of pure iron or heavy iron alloys (Fe+Ni) and is shown in the right vertex of the ternary diagram. The maximum size for a semi-solid planet (not gaseous) is obtained if it is composed purely of ices and water and plots in the left corner. For a $1M_\oplus$ planet these extreme values are ∼4900 km and ∼9300 km. Simple formation constraints suggest that the minimum and maximum are not quite at the vertices (more realistic conditions see section 4.1). Terrestrial planets (no substantial water content) of $5M_\oplus$ are shown in Fig. 2 on the side connecting mantle and core only.

4. Results

We have calculated the ternary diagrams for planets with $1M_{\oplus}$, $2.5M_{\oplus}$, $5M_{\oplus}$, $7.5M_{\oplus}$ and $10M_{\oplus}$ showing the maximum and minimum radius for each planet and curves of constant radius. Figure 2 shows the different ternary diagrams. The same value for radius can be obtained through different combinations of core, mantle and H_2O contents showing degeneracy in composition.

4.1. Initial Conditions and Constraints on Bulk Compositions

Our interior model of a super-Earth planet could not be a random mixture of layers of different mineral, alloy, or compositional shells. This is so for at least two general reasons: differentiation and constraints in the proto-planetary disk abundances. Therefore we make two basic assumptions in this work. The first is that all our model planets have undergone differentiation. The second is that the relative elemental abundances are the same as those in the Solar System and the solar neighborhood. The first assumption is not restrictive since all the terrestrial planets and large satellites in the Solar System are known to be differentiated. The second assumption should also be adequate for the super-Earths that we expect to be discovered in the near future (close-by and in the pre-selected targets of the Kepler mission).

Thus, we consider three possible initial states for our models:

(1) formation and post-differentiation anywhere in the proto-planetary disk - the ratios of Si/Fe, O/Fe, etc. depend on T_{cond} and the amount of Fe incorporated in the mantle depends on the O locally available;

(2) formation as in (1), followed by a collisional stripping - then four initial states are possible: (a) pure iron alloy core; (b) core and mantle; (c) pure mantle; and (d) mantle and water ocean; and,

(3) formation as in (1) or (2), followed by water delivery - then two initial states are possible: (a) core, mantle, and water ocean, and (b) mantle and water ocean.

To explore the first scenario we consider that during formation, the building blocks of planets - volatiles, silicates and metals - condense out at different temperatures T_{cond}. As the nebula cools down the most refractory elements will condense out first. The first of the building blocks of planets to condense out are silicates at temperatures between 1750-1060K (Krot et al. 2005), followed by the metals (Fe, Ni) between 1450-1050K (Krot et al. 2005) and finally H_2O and other ices, depending on the pressure. The relative amounts of the

different major elements in solid planets are H at 74%, O at 1.07%, Fe at 0.1%, Si at 0.065% and Mg at 0.058%. We consider Si and Mg to be practically equally abundant. During the condensation sequence (for pressure $< 10^{-4}$bars), Si will condense before Fe. If Fe remains immiscible it will form the core during condensation and planet segregation. This is the end state scenario that yields the largest core possible for a planet. That is, a fixed ratio of Si/Fe of ~ 0.6. The mantle is effectively $MgO+SiO_2$ so that Si/Fe ratio can be used as a proxy for MMF/CMF. This line is shown in Fig. 1 as the lowest possible values for MMF/CMF. Any value above this line is plausible during formation because Fe can be incorporated in the mantle to form $(Mg_{1-x}$, Fe)$O+SiO_2$ (with $x = 0.1$ for Earth) depending on the redox conditions.

To explore the possibility of having a planet with a large core and H_2O layers and a small mantle we consider a scenario with a pure Fe embrio that acquires water from comet delivery, which is scenario (3) stated above. Comets have a dust/gas ratio of 1-2. As the comet delivers water (gas, volatile) it will at least deliver Si+Mg+Fe+O in the same proportions. We consider that the cometary dust is made up of Si, Mg, Fe and O and that the proportions of these elements are the same as in the solar nebula (or CI chondrites). Then the ratio of Si/H_2O that needs to be maintained is at least 0.23 by mass. Therefore, for every gram of water delivered to the Fe pure embrio, 0.23g of Si (that makes up the mantle) will be delivered also. This is the end state case that yields the lowest amount of MMF possible for a given IMF. This line shows the minimum amount of mantle formed as planetesimals get accreted and deliver water. Accompanying this amount of Si, is the amount of Fe that, if in solar abundances can also add mass to the core. Therefore the unshaded region in Fig. 1 shows the plausible compositions that reflect the solar nebula composition and cometary delivery constraints.

To explore scenario (2) mentioned above, we contemplate late-stage processes that might influence the final accretionary state of a planet starting from a 'normal' embrio. Any process that induces the escape of preferentially light elements (solar wind, gravitational escape) will deplete the planet from volatiles, H_2O and perhaps silicates forming terrestrial planets (core, mantle+core planets). Conversely, any process that targets heavy elements to be excluded from accretion (like formation of the Moon after the Mars-sized impact onto a proto-Earth (Canup 2004)) would deplete the planet from Fe and silicates forming a light planet (mantle, mantle+water ocean planets). It is difficult to imagine a process that would preferentially retain the heavy and light elements simultaneously and blow-off or prevent from accreting the medium density components (silicates).

Based on these arguments we expect that planets with large CMF and IMF and small or non-existent mantles are very unlikely. Thus, the shaded region in Fig 1 is unlikely to be

populated.

4.2. Maximum Radius for Terrestrial Planets

For a given planet, a threshold in radius exists such that larger values imply that the planet is ocean-like - has a substantial amount of water and ices and can not be completely rocky ((Valencia et al. 2007). This threshold radius can be identified as the largest iso-radius curve that intersects the terrestrial side on Fig 2. All the iso-curves to the left (bluer region) of this curve show IMF>0. This threshold in radius is 6600 km, 8600km, 10400 km, 11600km and 12200km for $1M_{\oplus}$, $2.5M_{\oplus}$, $5M_{\oplus}$, $7.5M_{\oplus}$ and $10M_{\oplus}$ planets respectively. Thus, for a given planetary mass, a measurement in radius larger than its corresponding terrestrial threshold radius would imply that the planet either formed beyond the snow line acquiring large amounts of H_2O, or had large amounts of volatiles delivered to it by wet planetesimals.

The identification of the composition via this maximum terrestrial radius will be easier for smaller planets since their iso-curves are more significantly separated in the ternary diagram.

4.3. Iso-radius curves

Figure 2 shows the progression in radius from a $10M_{\oplus}$ to a $1M_{\oplus}$ planet and how the iso-radius curves move closer to each other as the mass increases. The lines of constant radius are less sensitive to the amount of mantle mass, illustrated in how parallel they lay with respect to increasing values of mantle percentage (iso-curves almost vertical).

- This is particularily true for a $5M_{\oplus}$ planet: a large range of mantle mass (between $0 - 85\%$) may yield the same radius of $\sim$ 11300km, provided the correct amount of water is present (from 50% to 15% respectively).
- For a $1M_{\oplus}$ planet, the iso-radius curves are tilted to be slightly more sensitive to mantle mass, less sensitive to the amount of core and more sensitive to water content (iso-cuves are more parallel to the lines of constant water content). At this pressure regime (smallest planet shown), the amount of low density (water) and high density (Fe) material can proportionally affect the total radius.
- For the case of a $10M_{\oplus}$ (high internal pressures) the iso-curves show that for very water rich planets ($> 70\%$ H_2O), the radius is dependent on the amount of core-mass

fraction (blue lines moving towards being parallel to the terrestrial line) and become less independent as the composition becomes iron rich (> 70% Core). For the large core fractions, the amount of water is important because the contrast in density is the largest. The overall trend is that the iso-radius curves are less sensitive to the amount of mass in silicate form (mantle) and the result for radius depends more in the amount of light elements (water and ices) and heavy elements (core-Fe).

There have been useful mass-radius relationships obtained with zero-temperature sphere models (Zapolsky & Salpeter 1969; Stevenson 1982; Fortney et al. 2006) that hint to the bulk composition of a planet. These models find the radii for different pure compositions such as H_2O, silicates or Fe. These radii (as a function of mass) correspond to each vertex of our ternary diagram. They also mix pairs of the above compositions, essentially following the sides of the ternary diagram. It can be seen from Fig. 2 that the iso-radius curves are very sensitive to the mixture and how they intersect with the ternary sides depends on it, especially in a mantle-H_2O mixture. Of course, the zero-temperature sphere models have no layering, or phase transitions, or convective mixing in the planet's interior. They also do not access the parameter space inside the ternary diagram. Therefore, a zero-temperature model is a good first approximation. However, detailed calculations are needed to distinguish between realistic compositions at the precision CoRoT and *Kepler* will allow.

5. Mass-Radius Relationship

We had previously stated that the radius of a super-Earth scales in a power law relationship with mass: $R = aR_\oplus \left(\frac{M}{M_\oplus}\right)^\beta$ where $a = 1$ and $\beta \sim 0.27$. We have improved this result by choosing an equation of state better suited for high-pressure extrapolations (Vinet EOS) and including the recently discovered new silicate phase - post-perovskite (ppv) in the Earth's lower-most mantle (Murakami et al. 2004). Even though the stability field of ppv is only of $\sim$ 10GPa on Earth, it constitutes most of the mantle of super-Earths. It also can accomodate more Fe in its structure than perovskite (Mao et al. 2004) making it more dense. With these improvements the exponent of the power law becomes smaller: $\beta = 0.262$. It is different from 1/3 - the constant density scaling value - due mostly to pressure effects. The scaling is independent of temperature effects (such as surface temperature, constant versus temperature-dependent viscosity cases), and CMF. It also differs little with core composition.

Sotin et. al (Sotin et al. 2007) has shown that planets that have 50% water content scale as $R = 1.25 \times R_\oplus \left(\frac{M}{M_\oplus}\right)^{0.274}$ for a family of planets that have the same Fe/Si ratio. Here, we generalize the power law relation for low-mass planets to include up to 50% H_2O

assuming a fixed ratio between the silicate and metal portion of a planet. Meaning, that the mantle and core mass fractions are the same so that the Fe/Si ratio of the family of planets with different IMF varies little. Figure 3 shows the radius as a function of mass in terms of Earth-masses for rocky and ocean planets. The generalization of the power law becomes

$$R_p = (1 + 0.56 \times \mathrm{IMF})\, R_\oplus \left(\frac{M_p}{M_\oplus}\right)^{0.262(1-0.138\times \mathrm{IMF})}$$

where IMF denotes the amount of water in percentage. Table 1 shows the values for the coefficient and the exponent in the power law corresponding to the family of planets with 0 up to 50% H_2O. The coefficient a shows how much larger Earth would be if it had different amounts of water. Earth would have an increase of 26% in radius if it had 50% water by mass. Our result for a 50% H_2O-planet differ from the exponent obtained by Sotin et. al. possibly because we include the newly discovered post-perovskite phase in the lower mantle (Murakami et al. 2004) and our preference for the Vinet EOS over the BM3 EOS chosen by Sotin et. al. We are presently working towards an understanding of this difference.

Figure 3 shows the mass-radius relationship for planets with a fixed mantle-to-core ratio of 2:1 as a proxy for Fe/Si. It also shows the relationship between the planetary mass and both the minimum and maximum radii. The minimum radius is obtained for a rocky planet with the largest possible core constrained from solar nebula composition. The maximum radius occurs when the planet is made of silicates and water constrained by the volatiles/Si ratio from chondritic material (refer to section 4.1).

6. Observational Characterization of Super-Earth Planets

The main result from our model calculations presented here is that there is a threshold of precision in R and M that allows bulk estimates of the composition χ. These are $\sim$5% in planetary radius and $\sim$ 10% in planetary mass (this is an average statement over the mass range $1 - 10 M_\oplus$ and our complete grid of models). Instrumentation currently under development will be able to provide such observational tolerances in the coming 5 years - in particular, the NASA *Kepler* mission in synergy with the HARPS-NEF spectrograph.

The *Kepler* mission (Borucki et al. 2003) will monitor a single field in Cygnus/Lyra and discover many hundreds of transiting planets orbiting preselected main-sequence stars (F to M-type) of 11th to 15th magnitude in V. It is capable of detecting more than 50 Earth-sized ($1 R_\oplus$) planets in all orbits, with about a dozen n orbits approaching 1-year period; as well as several hundred super-Earths ($\sim 1.3 R_\oplus$) in all orbits up to 1 year. The *Kepler* mission will achieve 20 ppm photometry or better on 12th magnitude stars (its "sweet spot" for detection).

The HARPS-NEF spectrograph is a collaborative Harvard-Geneva Observatory project to build and operate a high-precision radial velocity instrument in the Northern hemisphere for synergy with *Kepler*. Its design is based on that of HARPS (Pepe et al. 2005); it will be capable of achieving better than 1m/s in 1 hour on a 12th magnitude star of F- to M-type. That would allow planet mass determination of 10% or better for super-Earths (2-5 $_{\oplus}$) in orbits closer than 0.10 AU. For more massive super-Earths, 10% in mass is achieved for orbits up to 0.5 AU, all for planets already detected with transits by *Kepler*.

Using *Kepler* and HARPS-NEF together should allow tolerances in radius ($< 5\%$) and mass ($< 10\%$) for dozens of super-Earths, limited only by available observing time for HARPS-NEF. This would produce a large enough statistical sample to distinguish the bulk properties of ocean planets and dry rocky planets and their rate of occurance in orbits closer than ∼1AU. Examples of the ability to distinguish these properties are given in Fig.4 and 5.

Our estimate of 4% uncertainty in planet radius from *Kepler* incorporates the photometric uncertainty for 10 high-impact transits on a 12th magnitude star and the uncertainty in the stellar parameters (Cody & Sasselov 2002), and stellar radius in particular. This estimate makes use of the fact that *Kepler* will discover a large number of planets and only a sub-sample of the most suitable ones will be followed-up with HARPS-NEF and will have *Kepler*-derived parallaxes. A good general discussion of observational uncertainties for both CoRoT and *Kepler* is given by Selsis et al. (2007).

The apparent radius of a transiting planet depends on its atmosphere; Burrows et al. (2003) have estimated a several percent increase in the radius of a hot Jupiter compared to a reference radius at 1 bar pressure. We have neglected this 'transit radius' effect here, but note that it could be important for super-Earths with significant atmospheres.

7. Conclusions

We have present here the relationship between planetary mass, radius and bulk composition for planets in the $1M_{\oplus}$ to $10M_{\oplus}$ range. The main bulk composition materials can be described well in three groups: core (Fe), mantle (silicates) and water (H_2O). Therefore the planet radius dependence on bulk composition for given mass is best illustrated with the help of a ternary diagram. The degeneracy in composition is illustrated in curves of constant radius. These iso-radius curves are less sensitive to mantle composition, showing that the degeneracy is mostly achieved by a trade-off between core and H_2O content.

Our detailed models indicate that a maximum terrestrial radius exists for a given planetary mass - it separates dry rocky compositions from ones containing 10% or more water

by mass. A measured planet radius that exceeds that critical terrestrial radius would imply that the planet is an ocean planet. For the high-mass range, the possibility of a massive hydrogen-helium envelope has to be evaluated separately.

By considering realistic initial states for our interior models we can constrain the parameter space of plausible evolved models, as shown in Figs.1, 4, and 5. These constraints lead to minimum and maximum radius as a function of planet mass, and show that planets with small mantles and large core and H_2O contents are unlikely to form.

We provide a mass-radius relationship to include the effects of various amounts of water and note that the exponent β in $R = aR_\oplus \left(M/M_\oplus\right)^\beta$ decreases slightly as the amount of H_2O increases (due to the high compression of H_2O) and a increases almost linearly with H_2O content (due to the low density of H_2O).

8. Acknowledgments

We thank S. Jacobsen for fruitful discussions and the anonymous reviewer for his/her comments. D.V. is grateful for the support from the Harvard Origins of Life Initiative. This work was supported under NSF grant EAR 04-40017.

REFERENCES

Beaulieu, J. P., Bennett, D. P., Fouque, P., Williams, A., Dominik, M., Jorgensen, U. G., Kubas, D., Cassan, A., Coutures, C., Greenhill, J., Hill, K., Menzies, J., Sackett, P. D., Albrow, M., Brillant, S., Caldwell, J. A. R., Calitz, J. J., Cook, K. H., Corrales, E., Desort, M., Dieters, S., Dominis, D., Donatowicz, J., Hoffman, M., Kane, S., Marquette, J. B., Martin, R., Meintjes, P., Pollard, K., Sahu, K., Vinter, C., Wambsganss, J., Woller, K., Horne, K., Steele, I., Bramich, D., Burgdorf, M., Snodgrass, C., Bode, M., Udalski, A., Szymanski, M., Kubiak, M., Wieckowski, T., Pietrzynski, G., Soszynski, I., Szewczyk, O., Wyrzykowski, L., Paczynski, B., & Collaboration, T. M. 2006, Nature, 439, 437

Borde, P., Rouan, D., & Leger, A. 2003, ASTRON.ASTROPHYS., 405, 1137

Borucki, W. J., Koch, D., Basri, G., Brown, T., Caldwell, D., Devore, E., Dunham, E., Gautier, T., Geary, J., Gilliland, R., A.Gould, Howell, S., & Jenkins, J. 2003, in Proceedings of the Conference on Towards Other Earths: DARWIN/TPF and the Search for Extrasolar Terrestrial Planets, ESA SP-539, ed. M. Fridlund & T. Henning (Noordwijk), 69–81

Burrows, A., Sudarsky, D., & Hubbard, W. B. 2003, The Astrophysical Journal, 594, 545

Canup, R. M. 2004, Icarus, 168, 433

Cody, A. M., & Sasselov, D. D. 2002, ApJ, 569, 451

Cohen, R., O.Gulseren, & Hemley, R. J. 2000, Amer. Mineralogist, 85, 338

Ehrenreich, D., Etangs, A. L. D., Beaulieu, J.-P., & Grasset, O. 2006, ArXiv Astrophysics e-prints

Fortney, J. J., Marley, M. S., & Barnes, J. W. 2006, Planetary Radii across Five Orders of Magnitude in Mass and Stellar Insolation: Application to Transits

Hama, J., & Suito, K. 1996, J. Phys. Condens. Matter, 8, 67

Ida, S., & Lin, D. 2004, ApJ, 604, 388

Kennedy, G. M., Kenyon, S. J., & Bromley, B. C. 2006, The Astrophysical Journal, 650, L139

Krot, A. N., Scott, E. R. D., & Reipurth, B., eds. 2005, Meteoritic Constraints on Temperatures, Pressures, Cooling Rates, Chemical Compositions, and Modes of Condensation in the Solar Nebula, ed. A. N. Krot, E. R. D. Scott, & B. Reipurth, Vol. 341, 373–405

Table 1. Generalized mass-radius relationship – $R = aR_{\oplus}(\frac{M}{M_{\oplus}})^{\beta}$

H_2O	a	β
0	1	0.262
10	1.076	0.260
20	1.130	0.257
30	1.178	0.252
40	1.223	0.248
50	1.265	0.244

Note. — Values in the power law relationship between mass and radius of a super-Earth with similar Fe/Si ratio to Earth's

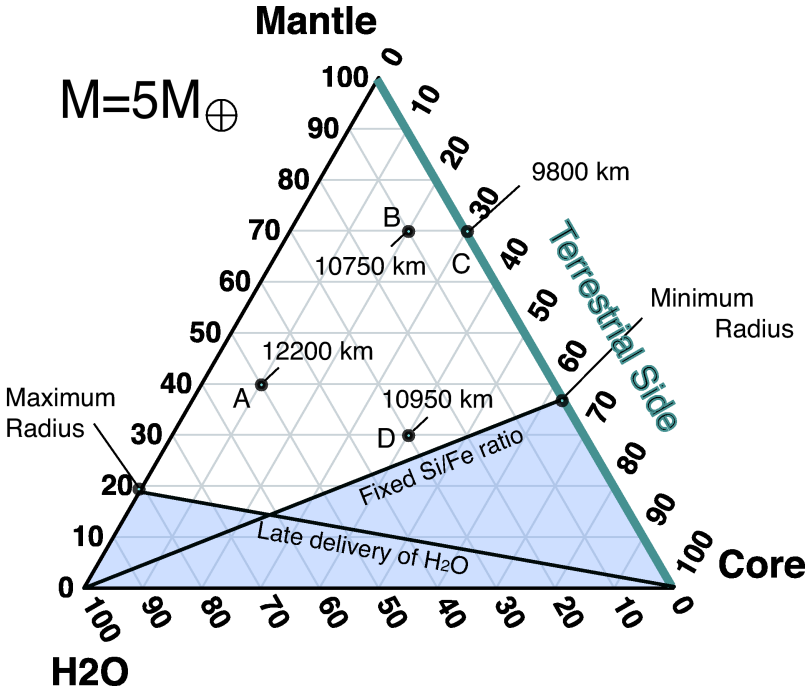

Fig. 1.— Ternary Diagram. The possible compositions of a super-Earth and radius are illustrated in a ternary diagram that depicts three axis: amount of H_2O, core (Fe) and mantle (silicates). Each point inside the triangle uniquely specifies a bulk composition and the corresponding radius - a few examples are labeled. The terrestrial side is the location where rocky planets would be shown. The minimum plausible radius is achieved with the largest core possible from solar nebula composition constraints and no water. The maximum plausible radius is shown for a planet with no core and maximum amount of water under the solar nebula composition constraints. The shaded region shows improbably compositions from solar nebula abundances and accretion processes.

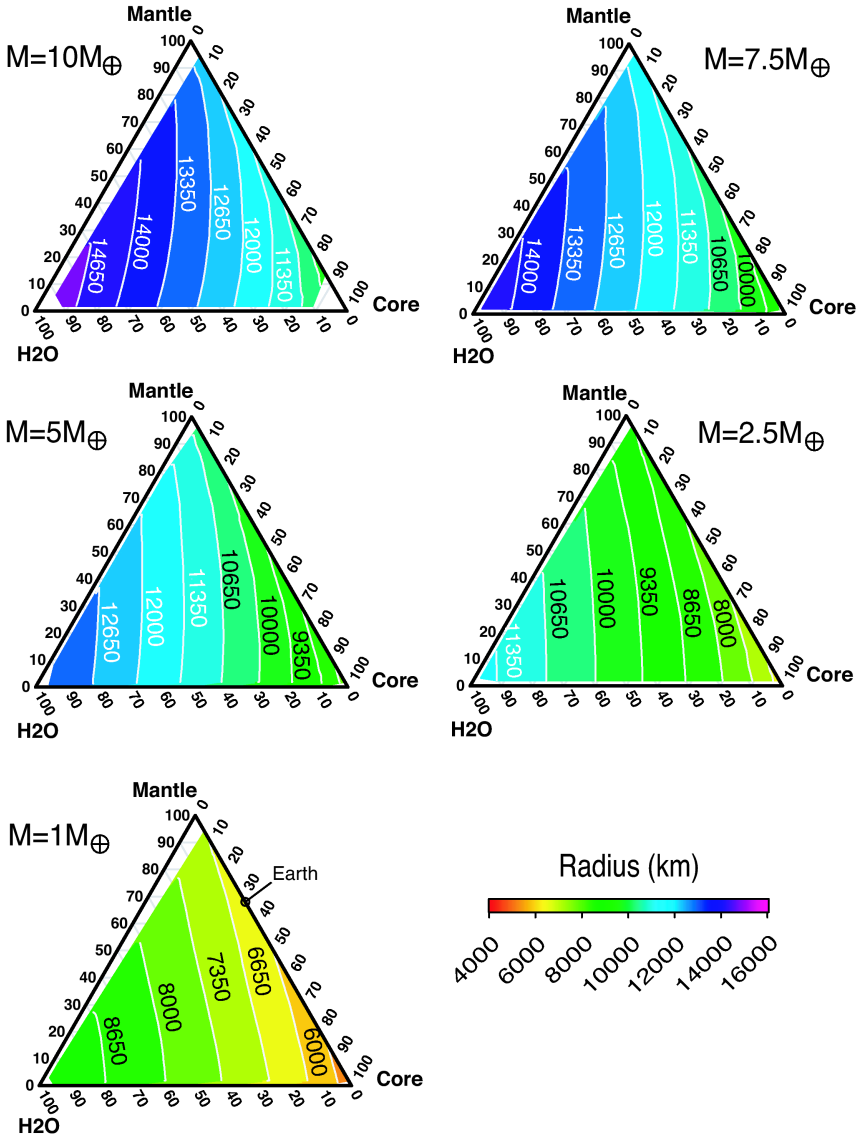

Fig. 2.— Ternary Diagram relating M, R, and χ. The iso-radius curves for possible bulk compositions are shown for a $10M_{\oplus}$, $7.5M_{\oplus}$, $5M_{\oplus}$, $2.5M_{\oplus}$ and $1M_{\oplus}$. As mass increases, the iso-radius curves shift to the right and rotate slightly. The progression from a 5000km ($1M_{\oplus}$ Fe-) planet to a 16000km ($10M_{\oplus}$ water-) planet is illustrated in the color bar. White regions on the ternary diagrams are areas that pose a numerical challenge on the model.

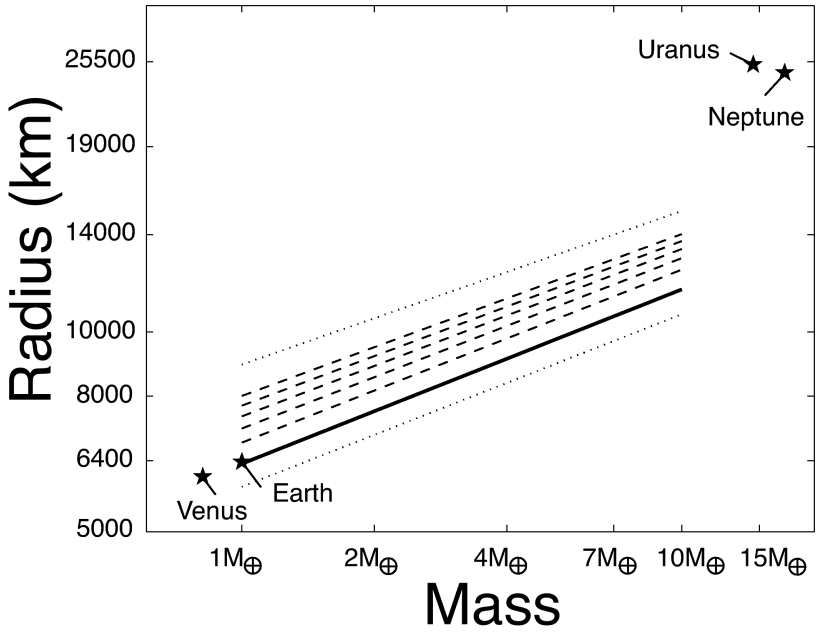

Fig. 3.— Mass-Radius relationship for Ocean and Rocky Massive Planets. The solid black line is the power law relationship for completely terrestrial planets with 1-10$M_{\oplus}$. The dashed lines above progressively represent the relationship for planets with 10%, 20%, 30%, 40% and 50% H_2O. This family of planets have a fixed mantle to core proportion of 2:1. The minimum and maximum planetary radius relations with mass are shown as dotted lines. Venus, Earth, Uranus and Neptune are shown for reference.

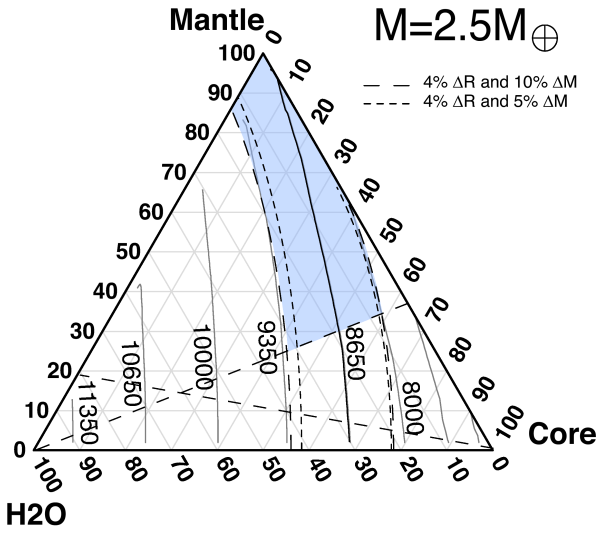

Fig. 4.— *Kepler* and HARPS-NEF capabilities for a 2.5 $M_\oplus$ planet. The shaded area around the terrestrial radius threshold illustrates the uncertainty from a 4% error in radius measurements and 5% (short-dashed line) and 10% (long-dashed line) error mass measurements. The range of possible interior structures (bulk compositions) is dominated by the radius uncertainty in this range of masses. The two dashed lines define interior structures excluded by the initial conditions - see Fig.1.

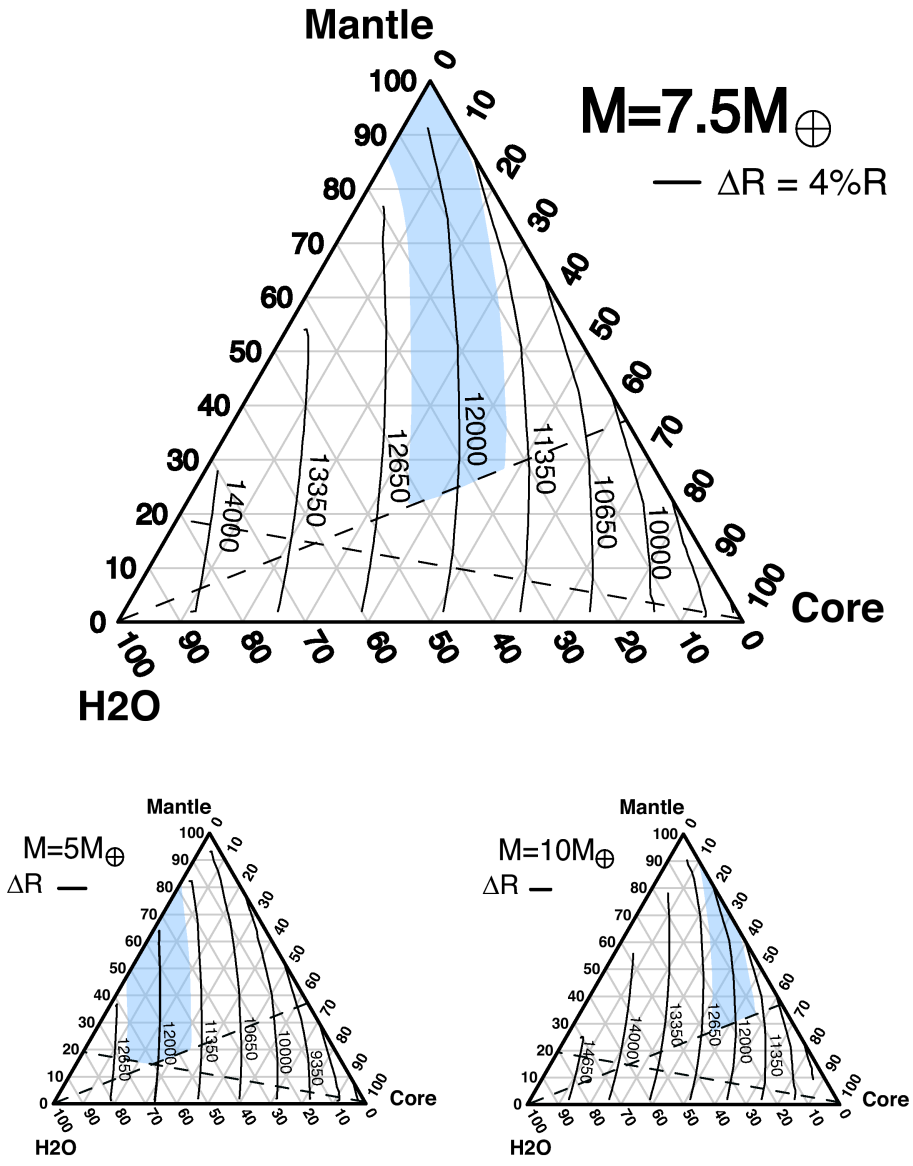

Fig. 5.— The shaded area around the terrestrial threshold radius illustrates a 4% error in radius measurement for a $7.5M_{\oplus}$ planet. The effect of uncertainty in planet mass measurement is illustrated in the bottom panel: the same radius value of 12000 km could correspond to very different compositions, if the planet mass is not known to better than 30%. In such a case it is not possible to determine whether the planet is an ocean planet or a dry rocky planet. The two dashed lines define interior structures excluded by the initial conditions - see Fig.1.

Kuchner, M. J. 2003, The Astrophysical Journal, 596, L105

Leger, A., Selsis, F., Guillot, C. S. T., Despois, D., Mawet, D., Ollivier, M., Labeque, A., Valette, C., B., F. B., Chazelas, & Lammer, H. 2004, Icarus, 169, 499

Lovis, C., M.Mayor, Pepe, F., Alibert, Y., Benz, W., Bouchy, F., Correia, A. C. M., Laskar, J., Mordasini, C., Queloz, D., Santos, N. C., Udry, S., Bertaux, J., & Sivan, J. 2006, Nature, 441, 305

Mao, W. L., Shen, G., Prakapenka, V. B., Meng, Y., Campbell, A. J., Heinz, D. L., Shu, J., Hemley, R. J., & Mao, H.-k. 2004, PNAS, 101, 15867

Murakami, M., Hirose, K., Kawamura, K., Sata, N., & Ohishi, Y. 2004, Science, 304, 855

Pepe, F., Mayor, M., Queloz, D., Benze, W., Bertaux, J.-L., Bouchy, F., Lovis, C., Mordasin, C., Santos, N., Sivan, J.-P., & Udry, S. 2005, The Messenger, 120, 22

Rafikov, R. R. 2006, Convective cooling and fragmentation of gravitationally unstable disks

Raymond, S. N., Mandell, A. M., & Sigurdsson, S. 2006, Science, 313, 1413

Rivera, E. J., Lissauer, J. J., Butler, R. P., Marcy, G., Vogt, S. S., Fischer, D. A., Brown, T. M., Laughlin, G., & Henry, G. W. 2005, ApJ, 634, 625

Selsis, F., Chazelas, B., Borde, P., Ollivier, M., Brachet, F., Decaudin, M., Bouchy, F., Ehrenreich, D., Griessmeier, J. M., Lammer, H., Sotin, C., Grasset, O., Moutou, C., Barge, P., Deleuil, M., Mawet, D., Despois, D., Kasting, J. F., & Leger, A. 2007, ArXiv Astrophysics e-prints

Sotin, C., Grasset, O., & Mocquet, A. 2007, Mass-Radius curve for extrasolar Earth-like planets and ocean planets

Stacey, F. 1992, in Physics of the Earth (Brookfield Press), 331–335

Stevenson, D. J. 1982, Planet. Sp. Sci, 30, 755

Valencia, D., O'Connell, R. J., & Sasselov, D. D. 2006, Icarus, 181, 545

Valencia, D., Sasselov, D. D., & O'Connell, R. J. 2007, ApJ, 656, 545

Vinet, P., Rose, J., Ferrante, J., & Smith, J. 1989, J. Phys. Cond. Matter, 1, 1941

Wagner, W., & Pruss, A. 2002, J. Phys. Chem. Ref. Data, 31, 387, doi:10.1063/1.11461829

Zapolsky, H. S., & Salpeter, E. E. 1969, ApJ, 158, 809